



HAL
open science

Influence of the Amazon-Orinoco Discharge Interannual Variability on the Western Tropical Atlantic Salinity and Temperature

M. Gévaudan, F. Durand, J. Jouanno

► **To cite this version:**

M. Gévaudan, F. Durand, J. Jouanno. Influence of the Amazon-Orinoco Discharge Interannual Variability on the Western Tropical Atlantic Salinity and Temperature. *Journal of Geophysical Research. Oceans*, 2022, 127, 10.1029/2022JC018495 . insu-03867917

HAL Id: insu-03867917

<https://insu.hal.science/insu-03867917>

Submitted on 23 Nov 2022

HAL is a multi-disciplinary open access archive for the deposit and dissemination of scientific research documents, whether they are published or not. The documents may come from teaching and research institutions in France or abroad, or from public or private research centers.

L'archive ouverte pluridisciplinaire **HAL**, est destinée au dépôt et à la diffusion de documents scientifiques de niveau recherche, publiés ou non, émanant des établissements d'enseignement et de recherche français ou étrangers, des laboratoires publics ou privés.



Distributed under a Creative Commons Attribution 4.0 International License

Key Points:

- A set of coupled ocean-atmosphere simulations is used to study the impact of Amazon interannual variability on the western tropical Atlantic
- Extreme floods of the Amazon impact significantly the sea surface salinity in the Amazon plume
- The sea surface temperature of the area is mostly influenced by the Atlantic Meridional Mode and not by the extreme floods of the Amazon

Correspondence to:

M. Gévaudan,
manon.gevaudan@gmail.com

Citation:

Gévaudan, M., Durand, F., & Jouanno, J. (2022). Influence of the Amazon-Orinoco discharge interannual variability on the western tropical Atlantic salinity and temperature. *Journal of Geophysical Research: Oceans*, 127, e2022JC018495. <https://doi.org/10.1029/2022JC018495>

Received 27 JAN 2022

Accepted 8 JUN 2022

Influence of the Amazon-Orinoco Discharge Interannual Variability on the Western Tropical Atlantic Salinity and Temperature

M. Gévaudan¹ , F. Durand^{1,2}, and J. Jouanno¹ 

¹LEGOS, Université de Toulouse, CNES-CNRS-IRD-UPS, Toulouse, France, ²Institute of Geosciences, University of Brasília, Brasília, Brazil

Abstract Over the last three decades, extreme floods have become increasingly frequent in the Amazon basin, affecting strongly the population and ecosystems of the area. However, the impact of these extreme events on the tropical Atlantic Ocean is still poorly known. In this study, we use a 1/4° coupled ocean-atmosphere model to assess the impact of the runoff interannual variability on the sea surface salinity and sea surface temperature of the area. Twin sensitivity experiments are performed, forced alternatively with interannually-varying and climatological river runoff. Composite fields for the highest floods and lowest floods are also compared. This combination of sensitivity tests and composite extremes allows to separate the effect of runoff interannual variability from the rest of the variability (typically driven by mixing, advection and precipitation). We show that the runoff interannual variability modulates the sea surface salinity of the Amazon plume with the same order of magnitude as the salinity variability driven by ocean dynamics and atmospheric forcing. However, due to vertical mixing, this oceanic imprint of the extreme floods is limited to a few months and a few hundred kilometers from the mouth. Years of extreme floods generally coincide with anomalous phases of the Atlantic Meridional Mode, which are associated with large-scale sea surface temperature anomalies over the tropical Atlantic Ocean. Our results did not reveal any significant modulation of these temperature anomalies by the runoff interannual variability, at any time of the year, questioning the relevance of a hydrological feedback on the tropical Atlantic sea surface temperature.

Plain Language Summary The Amazon River, the largest river in the world, regularly experiences extreme floods that strongly impact the population of the area. Moreover, these extreme events have become increasingly frequent in recent years because of the climate change already at stake. This study aims at understanding the impact of these extreme floods on the western tropical Atlantic Ocean, and especially on the salinity and the temperature of the region. To do so, we use a coupled ocean-atmosphere model of the tropical Atlantic Ocean, in which we include or discard the year-to-year variability of the river discharge. The comparison between the two simulations shows us that the extreme floods of the Amazon have a significant impact on regional salinity. However, despite the strong salinity change, the temperature does not seem to be affected by the Amazon floods.

1. Introduction

The Amazon basin is regularly affected by extreme droughts and floods, which have a strong impact on the population and the ecosystems of the region (e.g., Espinoza et al., 2016; Fassoni-Andrade et al., 2021; Filizola et al., 2014; Marengo et al., 2013). These extreme hydrological events are mainly associated with well-identified modes of tropical variability such as El Niño Southern Oscillation (ENSO) and the Atlantic Meridional Mode (AMM) (Drumond et al., 2014; Marengo & Espinoza, 2016; Towner et al., 2020). ENSO impacts the precipitation over South America, with El Niño events being generally associated with lower precipitation and river discharge in most of the Amazon basin while La Niña events are associated with higher precipitation and river discharge in the basin (e.g., Espinoza, Ronchail, et al., 2009; Ronchail et al., 2005; Ropelewski & Halpert, 1987; Towner et al., 2020). The influence of AMM on the extreme events of Amazon discharge is similar in magnitude to that of ENSO (Yoon & Zeng, 2010; Zeng et al., 2008). The positive AMM phase is linked to a decrease in the trade winds, a sea surface temperature (SST) increase in the North tropical Atlantic and a northward shift of the intertropical convergence zone (ITCZ), leading to a decrease in precipitation and therefore drought in the Amazon

© 2022. The Authors.

This is an open access article under the terms of the [Creative Commons Attribution License](https://creativecommons.org/licenses/by/4.0/), which permits use, distribution and reproduction in any medium, provided the original work is properly cited.

basin (Marengo et al., 2008, 2011; Xie & Carton, 2004). Conversely, the negative AMM phase is linked to a SST increase in the South tropical Atlantic and a southward shift of the ITCZ, leading to floods in the Amazon basin.

Over the last three decades, the hydrological cycle of the Amazon basin has intensified and extreme hydrological events are more frequent than in the early twentieth century (Barichivich et al., 2018; Espinoza, Guyot, et al., 2009; Gloor et al., 2013; Marengo & Espinoza, 2016). This intensification of the hydrological cycle is characterized by both a decrease of precipitation and river runoff during the dry season and an increase in precipitation and river runoff during the wet season (Espinoza, Guyot, et al., 2009; Espinoza, Ronchail, et al., 2009; Gloor et al., 2015, 2013; Liang et al., 2020). It is probably due to a warming trend in the tropical Atlantic, leading to a cooling of the eastern tropical Pacific, a strengthening of the Walker circulation and an enhancement of the moisture flux from the tropical Atlantic Ocean to the Amazon basin (Barichivich et al., 2018; Friedman et al., 2021; Li et al., 2016; McGregor et al., 2014; Wang et al., 2018).

The impact of the Amazon runoff on the tropical Atlantic Ocean has been largely studied. A common way of doing so is by using ocean circulation models in which the Amazon runoff is alternatively included or removed (Coles et al., 2013; Hernandez et al., 2016; Huang & Mehta, 2010; Jahfer et al., 2017, 2020; Masson & Delecluse, 2001; Newinger & Toumi, 2015; Varona et al., 2019). The other usual way is to analyze satellite and in-situ observations (Ffield, 2007; Fournier et al., 2017; Pailler et al., 1999; Zeng et al., 2008). Both observational and modeling studies concluded to a strong impact of Amazon runoff on the sea surface salinity (SSS), the salinity stratification and the plume extent. However, the SSS and the plume extent seasonal cycles are not caused by the seasonal cycle of Amazon runoff but by the seasonal cycle of the oceanic circulation (Coles et al., 2013; Masson & Delecluse, 2001). The impact of the Amazon runoff on the tropical Atlantic SST is controversial, with observational studies suggesting a strong impact on SST (Ffield, 2007; Fournier et al., 2017; Jury, 2019; Pailler et al., 1999) while modeling studies find a weak impact on SST (Coles et al., 2013; Hernandez et al., 2016; Huang & Mehta, 2010; Jahfer et al., 2017, 2020; Masson & Delecluse, 2001; Newinger & Toumi, 2015; Varona et al., 2019). Moreover, the Amazon plume region is regularly crossed by a large number of cyclones, and the influence of the Amazon plume on the development and the intensification of these cyclones is still under debate (e.g., Balaguru et al., 2012, 2020; Hernandez et al., 2016; Newinger & Toumi, 2015; Yan et al., 2017).

The impact of the Amazon runoff interannual variability has been less extensively studied, with published results that can appear contradictory. Several studies have found a link between the variability of Amazon runoff and the SSS variability of different areas: Barbados (Hellweger & Gordon, 2002), the Antilles (Jury, 2019), the north-equatorial countercurrent (NECC, Gouveia et al., 2019), and along the Amazon plume trajectory (Salisbury et al., 2011). However, Grodsky et al. (2014) observed that the ocean surface was saltier in 2012, despite a stronger Amazon runoff this year, and Fournier et al. (2017) found no evidence of a river discharge influence on SSS east of the lesser Antilles. Moreover, the modeling study of Grodsky et al. (2015) found a SSS variability in the Caribbean Sea very close to observations while their model considered a climatological runoff, leading them to conclude that the interannual variability of the Amazon does not have a significant impact on the SSS interannual variability in this area. Regarding SST, a positive correlation is found between the interannual variability of the Lesser Antilles SST and the Amazon runoff (Jury, 2019), and between the SST and the SSS to the east of the Lesser Antilles (Fournier et al., 2017). However, Fournier et al. (2017) also mention a strong interannual variability of SST linked with the AMM that could impact these results.

The studies on the impact of the interannual variability of the Amazon discharge were usually conducted with ocean observations, which present several problems. One of them is that the correlations found are highly dependent on the discharge estimates used (Reeves Eyre & Zeng, 2021), and that the Óbidos stream gauge commonly used to estimate the Amazon discharge at the river mouth misrepresents the seasonal cycle (Reeves Eyre & Zeng, 2021; Salisbury et al., 2011). Another one is that the oceanic impact of runoff variability cannot be separated from the impact of ocean and atmospheric variability (mixing, advection, atmospheric fluxes), something that can be done with a model. To our knowledge, no sensitivity test has ever been conducted with a model to isolate the impact of runoff interannual variability on the Amazon plume region. This is therefore the aim of this paper: to quantify the impact of runoff interannual variability on the SSS and SST of the region. To address this question, we used a regional ocean–atmosphere coupled model of the tropical Atlantic Ocean with a $1/4^\circ$ resolution. The use of a coupled model is essential since we want to assess changes in the ocean thermodynamics as a whole, including SST. Indeed, the ocean–atmosphere interactions are very strong in this area, and all the processes at stake would not be correctly represented in an ocean model forced with a prescribed atmosphere (Gévaudan et al., 2021). We

analyze two long-term simulations (2001–2015), forced alternatively with daily interannually-varying runoff and a daily runoff climatology. We focus on the flood season. A composite analysis of the years with abnormally high and abnormally low floods for both simulations allows us to isolate and quantify precisely the effect of the extreme floods that occurred in the last decades, and separate the effect of runoff interannual variability from the effects of ocean and atmospheric interannual variability.

2. Methodology

2.1. Coupled Model Description

The coupled configuration uses the ocean model NEMO v4.0 (Nucleus for European Modeling of the Ocean; Madec & the NEMO team, 2016), the atmospheric model WRF-ARW v3.7.1 (Weather Research and Forecasting; Skamarock & Klemp, 2008) and the coupler OASIS3-MCT v4.0 (Craig et al., 2017). The ocean and atmospheric models share a same Arakawa-C grid, extending from 15°S to 35°N, and from 99°W to 20°E, with a resolution of 1/4° (~27 km at the equator) and a Mercator projection. MERCATOR-OCEAN daily global reanalysis GLORYS2v4 (Ferry et al., 2012) is used to prescribe the lateral boundaries of the ocean model, while 6-hourly fields from ERA-Interim reanalysis (Dee et al., 2011) are used to force the lateral boundaries of the atmospheric model. This coupled model has already been used by Gévaudan et al. (2021), and the ocean configuration has been developed by Giffard et al. (2019). The reader is referred to these two papers for further details on the configurations, and for a comprehensive validation of the coupled model mean state. Note that the ocean color forcing of the solar radiation penetration scheme has been modified. Following Hernandez et al. (2017), we use global daily filled chlorophyll data from GlobColour 009_082 (Garneison et al., 2019; Maritorea et al., 2010), which is based on a merging of several satellite products, and the empirical parameterization from Morel and Berthon (1989) to calculate a vertical profile of chlorophyll from surface chlorophyll satellite concentration.

2.2. Simulations

The ocean component of the coupled model is initialized from World Ocean Atlas (Locarnini et al., 2018; Zweng et al., 2019), and then spun up alone from 1970 to 1999 using DFS5.2 atmospheric forcing (Dussin et al., 2016) with a bulk formulation (Large & Yeager, 2009). Two coupled simulations of 16 years each are then conducted, with the last 15 years—from 2001 to 2015—being analyzed. The aim of these twin experiments is to assess the impact of the runoff interannual variability. Therefore, the first simulation, REF, has interannual daily runoff forcing while the second simulation, CLIM, has a daily climatological runoff forcing averaged from 2001 to 2015. Runoff data were obtained from the ISBA-CTRIP land surface model (Decharme et al., 2019). Their reliability to properly represent the large river plume properties of the tropical Atlantic was assessed in Giffard et al. (2019). Moreover, Newinger and Toumi (2015) showed that the highly turbid waters of the Amazon plume prevent the sunlight from reaching the deeper ocean, enhancing the warming of the surface layer and simultaneously limiting the warming of the subsurface layer. The ocean color is thus of great importance in the good representation of the impact of Amazon plume on the air-sea heat fluxes. Therefore, we decided to use chlorophyll fields consistent with the runoff forcing: we used interannual daily fields of chlorophyll for the REF experiment, and a daily climatology averaged from 2001 to 2015 for the CLIM experiment.

2.3. Validation

The mean state of the model has already been extensively validated in Gévaudan et al. (2021). Therefore, we only assess the ability of the model to reproduce the mean state and the interannual variability of the regional salinity. For this purpose, we used observed spaceborne salinity data from the Climate Change Initiative project (CCI, Boutin et al., 2020) from 2010 to 2015, which is the common period between the model simulations and CCI data set. We also used in-situ salinity data from the Service d'Observation on Sea Surface Salinity (SO-SSS) network (Delcroix et al., 2002). In the Amazon plume, these data consist of thermosalinograph transects from ships plying bi-monthly between French Guiana (5°N, 53°W) and France, recorded between 2005 and 2015 (Alory et al., 2015). Figures 1a and 1b show the mean SSS for the REF simulation and for CCI respectively. The model is overall in good agreement with the observations, except for a slightly too high SSS in the subtropical gyre. In particular, the Amazon-Orinoco plume is well reproduced, apart from the fact that the plume extends a little too far into the Caribbean Sea. The lower SSS area in the central tropical Atlantic, associated with the ITCZ and the

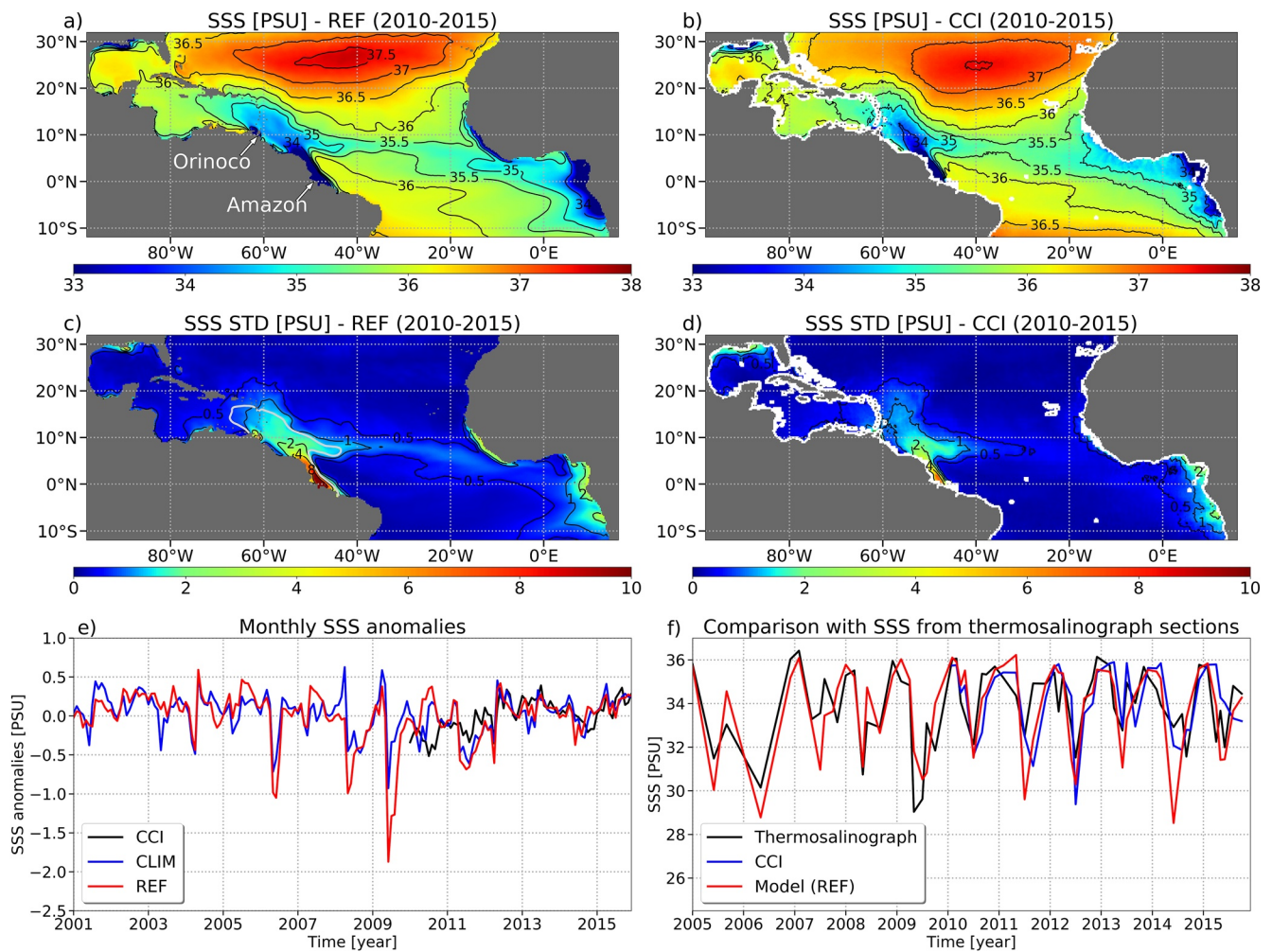


Figure 1. Maps from 2010 to 2015 for REF simulation of (a) sea surface salinity (SSS) mean and (c) monthly SSS standard deviation; (b) and (d): same as (a) and (c) respectively, but for Climate Change Initiative project (CCI) data; (e) time series of monthly SSS anomalies with respect to the monthly SSS climatology from 2010 to 2015 for REF (in red), CLIM (in blue) and CCI data (in black), averaged in the Amazon-Orinoco low salinity plume; (f) time series of SSS of in-situ data from thermosalinograph transects (in black), REF (in red) and CCI data (in blue), averaged on the thermosalinograph transects between 5°N and 10°N, and between 48°W and 53°W. The mouths of the Amazon and Orinoco rivers are indicated by arrows on (a). The white curve in (c) shows the 35 PSU mean SSS contour from 2001 to 2015, delineating the Amazon-Orinoco plume.

eastward transport of the Amazon-Orinoco plume by the NECC (e.g., Coles et al., 2013) is also well reproduced. Figures 1c and 1d show the standard deviation (STD) of monthly SSS for the REF simulation and for CCI respectively. The patterns are well reproduced by the model, but the interannual variability near the Amazon mouth is slightly higher in the model than in the observed data. Figure 1e shows SSS monthly anomalies with respect to a 2010–2015 SSS monthly climatology for REF (in red) and CCI (in black), averaged in the Amazon-Orinoco plume. The two time series are overall in good agreement from 2012 onwards. In 2010, the SSS peak in REF does not appear in CCI observations, even though it coincides with one of the most severe Amazon droughts ever recorded (e.g., Barichivich et al., 2018). Some salinity drops are also present in our model but not in the CCI observations (2011, 2014). These discrepancies can be due to the underestimation of SSS on the Amazon shelf in the model due to the too coarse resolution of the model and/or to the absence of tides (Ruault et al., 2020). They can also be caused by a lower accuracy of satellite data near the coast and in areas of high variability such as river plumes, despite an improvement of the algorithms in recent years (Boutin et al., 2018; Reul et al., 2020). Finally, we compare the model and CCI data with in-situ data from the thermosalinograph transects (Figure 1f). We can see that both the model and CCI data are in very good agreement with the in-situ measurements, which strengthens our confidence in the model to accurately reproduce the SSS variability, and underlines the progress made in salinity retrieval algorithms.

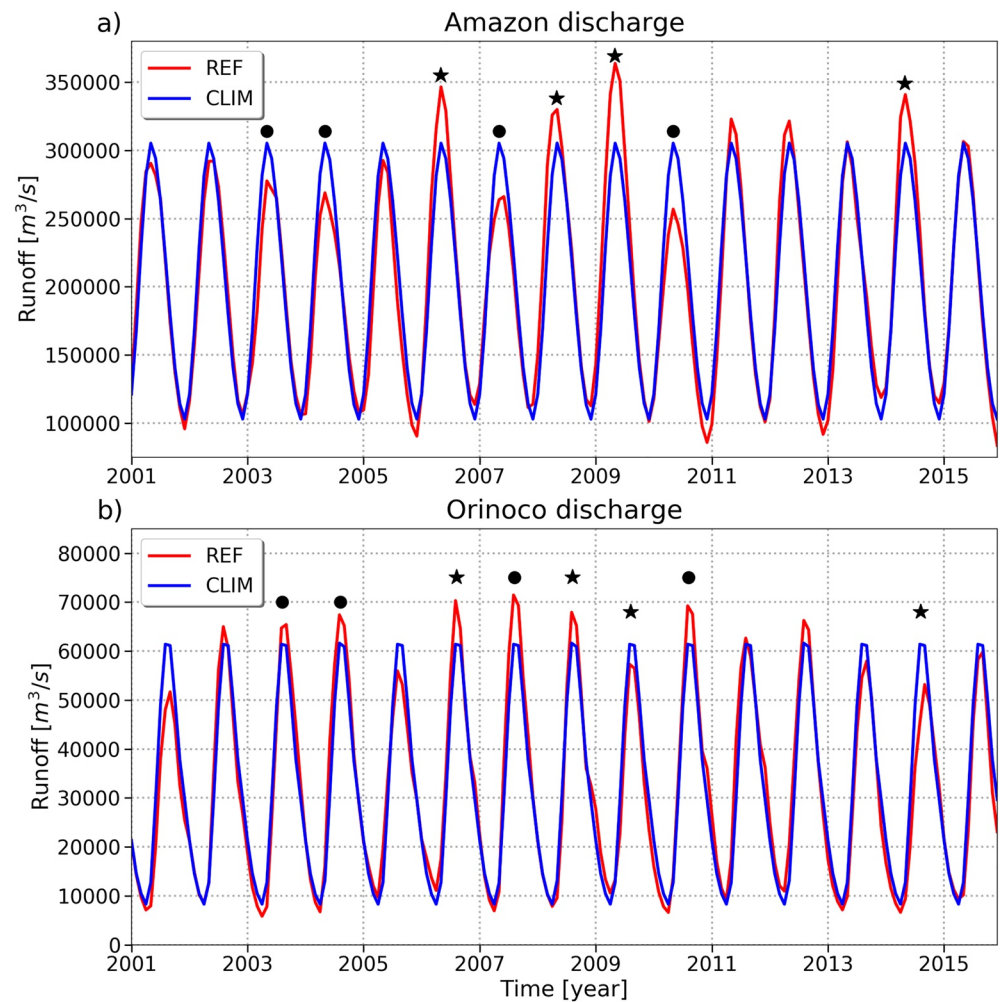


Figure 2. Time series of (a) Amazon and (b) Orinoco discharge for the REF and CLIM experiments. The dots indicate the years with the lowest Amazon floods while the stars indicate the years with the highest Amazon floods.

2.4. Methods

2.4.1. Composites Calculation

A composite analysis is conducted in the rest of the paper to analyze the consequences of the anomalous Amazon discharges during the flood season, resulting either from abnormally high floods or abnormally low floods, on the tropical Atlantic Ocean. Since the Amazon River has the largest discharge of the world and accounts for around 70% of the total discharge received by the northwestern tropical Atlantic, we based our composite analysis on the Amazon runoff, shown on Figure 2a. The 4 years with the highest floods, 2006, 2008, 2009 and 2014, are averaged to give the highest floods composite or HF, while the 4 years with the lowest floods, 2003, 2004, 2007 and 2010, are averaged to give the lowest floods composite, or LF. The years of highest and lowest floods are chosen by comparing the maximum discharge value of each year. We chose to study the flood season because the seasonal cycle of interannual discharge STD peaks at this time (not shown), indicating that variability is greater during this season. The composite analysis is performed on both REF and CLIM simulations. In the following, REF_{HF} and $CLIM_{HF}$ refer to the two composites for the highest floods years, and REF_{LF} and $CLIM_{LF}$ refer to the two composites for the lowest floods years. The seasonal maxima of runoff is around 345,000 m^3/s for REF_{HF} , around 267,000 m^3/s for REF_{LF} , and around 305,000 m^3/s for the CLIM experiment, giving a 25% relative change between the peak runoff of the REF_{HF} and REF_{LF} composites.

2.4.2. Differences Between Composites

In the following, differences between composites are analyzed. This allows to assess the impact of runoff interannual variability independently of the ocean and atmospheric variability (mixing, advection, atmospheric fluxes of freshwater and heat). The difference between REF_{HF} and REF_{LF} represents the sum of all variabilities: river runoff, ocean dynamics and atmospheric fluxes. The difference between $CLIM_{HF}$ and $CLIM_{LF}$ represents the impact of ocean and atmospheric variability only. Indeed, the river runoff is climatological in the CLIM experiment, which means that the runoff interannual variability is removed, leaving only the ocean and atmospheric variability. Therefore, the difference between REF and CLIM composites—that is $(REF_{HF} - REF_{LF}) - (CLIM_{HF} - CLIM_{LF})$ —represents the sole influence of runoff variability.

The error of these differences has been calculated as follows: the differences between composites have been calculated for all the individual years in pairs, giving 16 differences values. The STD of these 16 values has then been calculated, and represents the error.

2.4.3. Mixed Layer Salt Budget

A mixed layer salt budget was calculated online, and is expressed as follows:

$$\underbrace{\partial_t \langle S \rangle_h}_{\text{Total tendency}} = \underbrace{\langle -u\partial_x S - v\partial_y S \rangle_h}_{\text{Horizontal Advection}} + \underbrace{\langle D_l \rangle_h}_{\text{Lateral Diffusion}} + \underbrace{\frac{(E - P) \langle S \rangle_h}{h}}_{\text{Atmospheric Forcing}} + \underbrace{\langle -w\partial_z S \rangle_h}_{\text{Vertical Advection}} + \underbrace{\frac{(K_z \partial_z S)_{z=-h}}{h}}_{\text{Vertical Diffusion}} + \underbrace{\frac{\partial_t h}{h} (S_{-h} - \langle S \rangle_h)}_{\text{Entrainment}} \quad (1)$$

Vertical Processes

with

$$\langle \bullet \rangle_h = \frac{1}{h} \int_{-h}^0 \bullet \quad (2)$$

where S is the model salinity, u the zonal current, v the meridional current, w the vertical current, K_z the vertical diffusion coefficient and D_l the lateral diffusion. $E - P$ is the air-sea freshwater flux, with E the evaporation and P the precipitation. S_{-h} is the salinity at the mixed layer base, and h is the mixed layer depth (MLD). The MLD is computed as the depth where the density is equal to the 10-m density plus $\Delta\sigma$, with $\Delta\sigma = 0.01 \text{ kg/m}^3$ (de Boyer Montégut et al., 2007). Note that the river runoff is imposed as a divergence of the flow at the coastal point closest to the river mouth, and is therefore included in the advection term.

2.4.4. Definition of the Amazon-Orinoco Plume

In the following, some analyses are conducted in the low salinity plume associated with the Amazon and Orinoco rivers. Following Coles et al. (2013), the plume is defined as the area where the annual SSS averaged from 2001 to 2015 is under 35 PSU, and is shown in Figure 1c (white contour).

3. Results

3.1. Impact of Runoff Interannual Variability on SSS

The first aim of this study is to investigate the impact of the runoff interannual variability on SSS. The curves in Figure 3 represent the seasonal cycle of SSS in the Amazon-Orinoco plume in REF (solid lines) and CLIM (dashed lines) for the highest floods (blue lines) and lowest floods (red lines) composites. At the beginning of the year, SSS is similar for all composites. Then, as the flood season peaks, anomalies develop. For both REF and CLIM, the differences between highest floods and lowest floods years are the largest from mid-April to July. They subside afterward and have completely disappeared by October: the anomalies vanish in a few months only.

To quantify the impact of the runoff interannual variability on SSS, we now analyze differences between composites of SSS seasonal cycle (Figure 3, bar chart). As explained in Section 2.4.2, these differences allow to disentangle the different forcings driving the SSS anomalies. First, we can see that the change between the highest and

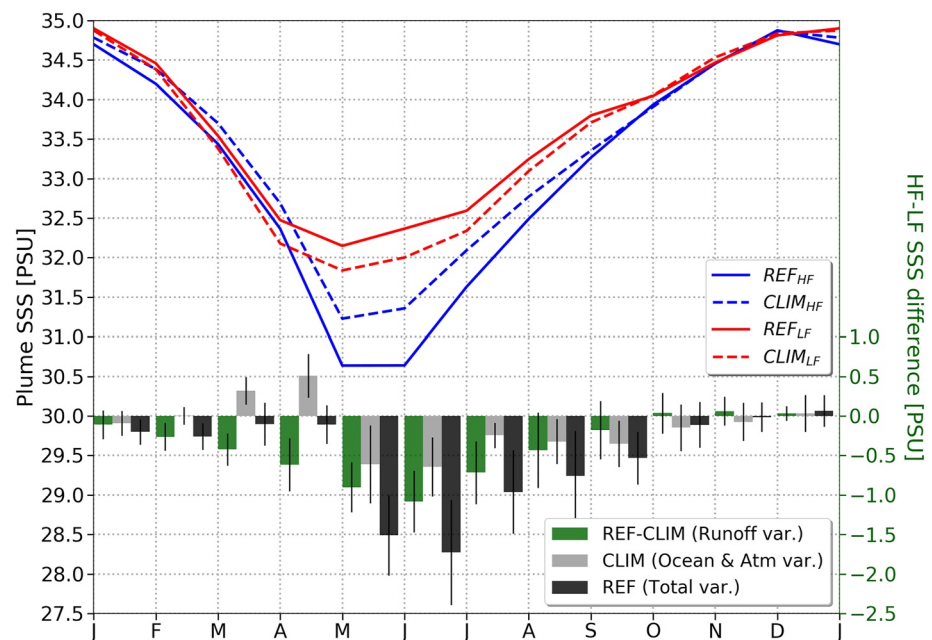


Figure 3. Sea surface salinity (SSS) seasonal cycle in the Amazon-Orinoco plume of each composite (curves) and of the differences between composites with their errors (bar chart).

lowest floods years when the whole variability is considered is very important in spring and summer: up to 1.7 PSU in June (Figure 3, black bars). This change is due almost equally to runoff interannual variability (Figure 3, green bars) and to ocean and atmospheric variability (Figure 3, gray bars), with nonetheless a larger share of the variability explained by runoff in May-June-July. This indicates that the interannual variability of the Amazon does not explain all of SSS variability in the region: other factors such as the surface currents (and especially the North Brazil Current, or NBC), the precipitation and the wind-induced mixing and currents influence the SSS variability in the same way as the runoff, reinforcing the fresh anomalies during the years of excess runoff (Coles et al., 2013; Fournier et al., 2017; Masson & Delecluse, 2001; Molleri et al., 2010). This result is in disagreement with Grodsky et al. (2014) and Grodsky et al. (2015), who suggested that runoff interannual variability has no impact on SSS variability. It stands therefore in agreement with the studies observing a correlation between SSS and runoff variabilities (Gouveia et al., 2019; Hellweger & Gordon, 2002; Jury, 2019; Salisbury et al., 2011).

Impacts are not expected to be similar between the near-shore and offshore portions of the plume. This is confirmed by maps of SSS difference between REF composites in spring (Figure 4a) and summer (Figure 4b), the two seasons of greatest change. A strong SSS decrease is observed in spring close to the river mouth and along the Guiana coast. In summer, the decrease has already partially vanished and has moved toward the lesser Antilles, while an increase in SSS is observed to the east, at the location of the NBC retroflexion and the NECC.

To quantify the part of SSS variability that can be attributed to runoff interannual variability, we now analyze maps of SSS difference between REF and CLIM composites for spring (Figure 4c) and summer (Figure 4d). In spring, the runoff interannual variability leads to an important freshening near the Amazon mouth (more than 3 PSU) and over the whole Amazon plume, decreasing with the distance from the mouth (more than 1 PSU up to 9°N and 0.2 PSU in the Lesser Antilles). In summer, the changes are still noticeable but their magnitude has diminished by a factor of 2–3.

The patterns of SSS differences driven by ocean and atmospheric variability are captured by the CLIM experiment (Figures 4e and 4f). In spring, the map of SSS difference between years of highest floods and years of lowest floods shows a dipole with positive anomalies near Guiana and in the Lesser Antilles, and a strong negative anomaly near the Amazon mouth. These anomalies are consistent with changes in the currents, as can be seen in Figure 4g. At this time of the year, the Amazon plume is mainly advected northwestward along the coast by the NBC and the Guiana current (Coles et al., 2013). Figure 4g shows a weakening of these currents in highest floods years compared to lowest floods years, leading on the one hand to an accumulation of freshwater near

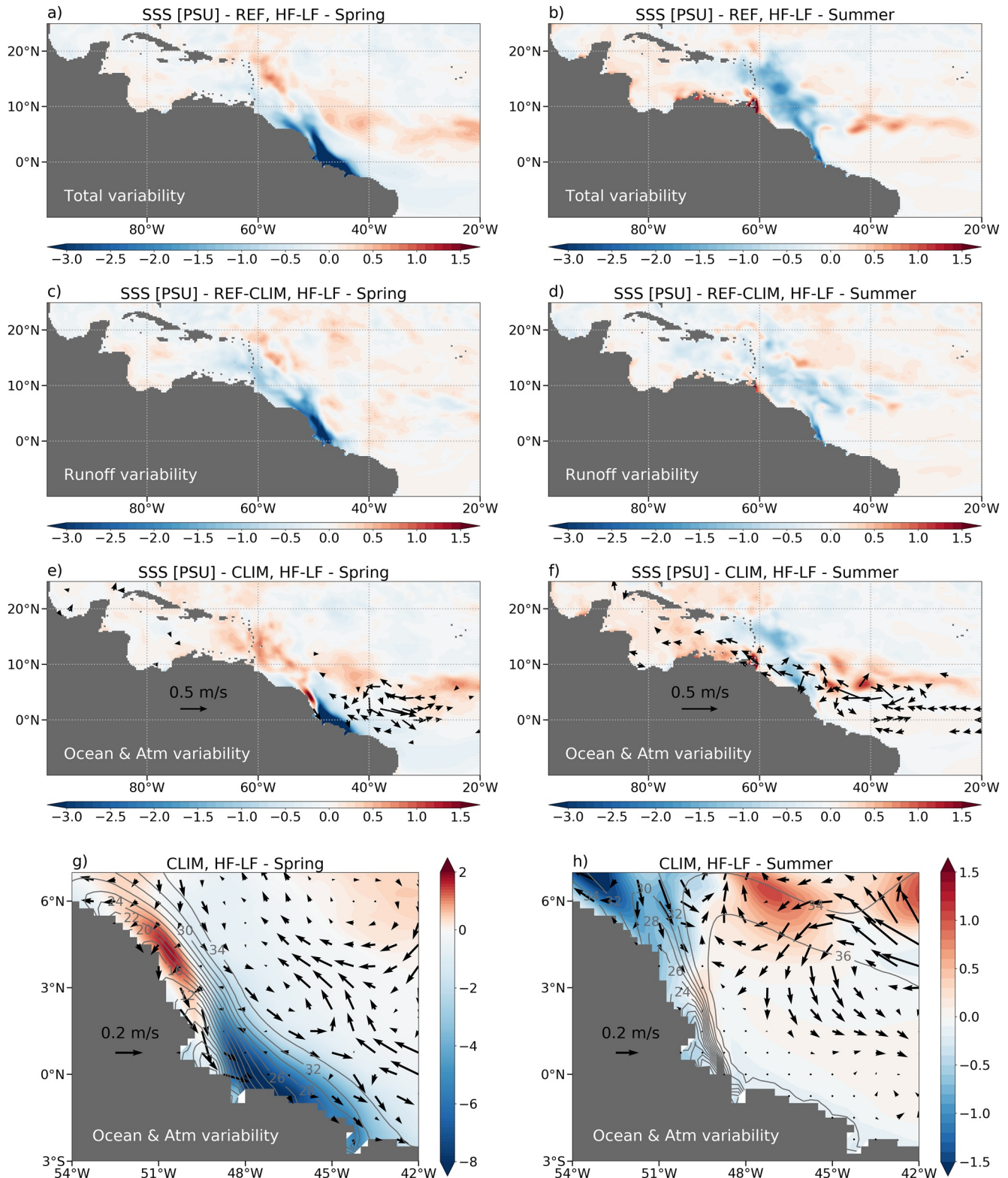


Figure 4. Spring (April-May-June, AMJ) maps of sea surface salinity (SSS) differences between highest floods and lowest floods composites for (a) REF, (c) REF – CLIM and (e) CLIM; (b, d and f): same as (a, c and e) respectively but for the summer season (July-August-September, JAS); the arrows on (e and f) represent the current anomalies with a norm greater than 0.1 m/s. (g and h): zoom at the Amazon mouth of (e and f) respectively. The contours represent the SSS of CLIM_{HF} (contours are every 2 PSU) and the arrows represent the currents anomalies of (CLIM_{HF} – CLIM_{LF}) for each season.

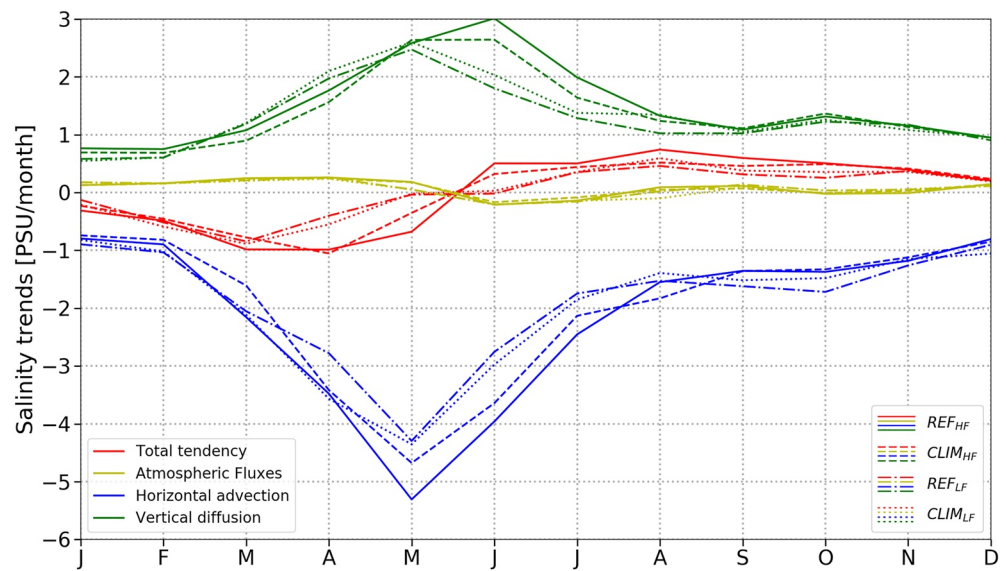


Figure 5. Seasonal cycle of the mixed layer salt budget in the Amazon-Orinoco plume.

the Amazon mouth, and on the other hand to a lesser northwestward along-shore freshwater transport and thus a positive SSS anomaly along the Guiana coast. Furthermore, these changes occur in the Amazon plume front region, an area of very strong SSS gradients (see contours of Figure 4g), which explains the high amplitude of the negative anomaly (down to -9 PSU). A southward shift of the NECC can also be observed (see arrows on Figure 4e). In summer, the anomaly of the currents near the Amazon mouth disappears (Figure 4h), as well as the SSS anomaly dipole. A strengthening of the NBC and a weakening of the NBC retroflection are observed (see arrows on Figure 4f), leading to an increase of freshwater transport toward the Lesser Antilles and a decrease of freshwater transport by the NECC. Finally, we note here again that the contribution of runoff interannual variability is similar in magnitude to the contribution of ocean and atmospheric variability in spring and summer.

To understand more precisely the changes in salinity observed, and especially the fast disappearance of the SSS anomaly (Figure 3), we analyze the seasonal cycle of mixed layer salt budget averaged over the Amazon-Orinoco plume (Figure 5). Two main processes dominate this salt budget: the horizontal advection and the vertical diffusion. The atmospheric freshwater fluxes (evaporation and precipitation) are negligible. The horizontal advection term is strongly negative since it corresponds to the transport of freshwater from the river runoff, and it dominates the total tendency at the beginning of the year. However, it is immediately counterbalanced by a strongly positive vertical diffusion term that mixes the underlying salty water into the ML. Therefore, the total tendency becomes positive as early as June. These results are consistent with Ferry and Reverdin (2004), who also found a strong contribution of horizontal advection at the beginning of the year, followed by a damping by vertical mixing and entrainment. It is also consistent with Foltz et al. (2004), who found that horizontal advection was an important component of the salt budget in the northwestern tropical Atlantic due to strong SSS gradients. Camara et al. (2015) found a more prominent effect of the vertical mixing year-round and lesser impact of horizontal advection, but their analysis domain lies further east and is not representative of the whole plume. Finally, if we observe the different curves on Figure 5 individually, we can see that the runoff interannual variability impacts the salt budget. In summer, the horizontal advection and vertical diffusion are stronger in REF_{HF} (solid lines) than in CLIM_{HF} (dashed lines): adding the runoff interannual variability exacerbates the response during the highest floods years (see also Table 1). Conversely, REF_{LF} (dashed-dotted lines) shows weaker horizontal advection and weaker vertical diffusion than CLIM_{LF} (dotted lines) in summer (see also Table 1). Note that the errors associated with some of the salinity budget terms are relatively

Table 1
Differences Between REF and CLIM Simulations and Their Associated Errors for the Two Main Terms of the Mixed Layer Salt Budget During Their Season of Maximum Change: The Vertical Diffusion (Averaged Between May and August, MJJA), and the Horizontal Advection (Averaged Between April and July, AMJJ)

| Salinity budget term | REF _{HF} – CLIM _{HF} | REF _{LF} – CLIM _{LF} |
|-----------------------------|--|--|
| Vertical diffusion (MJJA) | 0.19 ± 0.12 | -0.19 ± 0.11 |
| Horizontal advection (AMJJ) | -0.33 ± 0.20 | 0.30 ± 0.06 |

Note. The error is calculated as follows: the seasonal means are calculated for each year of the composites differences, giving 4 different values; the error is then calculated as the standard deviation of these 4 values.

large. For example, the error for the horizontal advection term is larger than the mean value. This is due to the high interannual variability of the runoff, which is not fully captured by the CLIM simulation. The error for the vertical diffusion term is also large, but it is smaller than the mean value. This is due to the high interannual variability of the vertical diffusion, which is not fully captured by the CLIM simulation. The error for the total tendency term is also large, but it is smaller than the mean value. This is due to the high interannual variability of the total tendency, which is not fully captured by the CLIM simulation. The error for the atmospheric fluxes term is very small, as expected, since it is negligible.

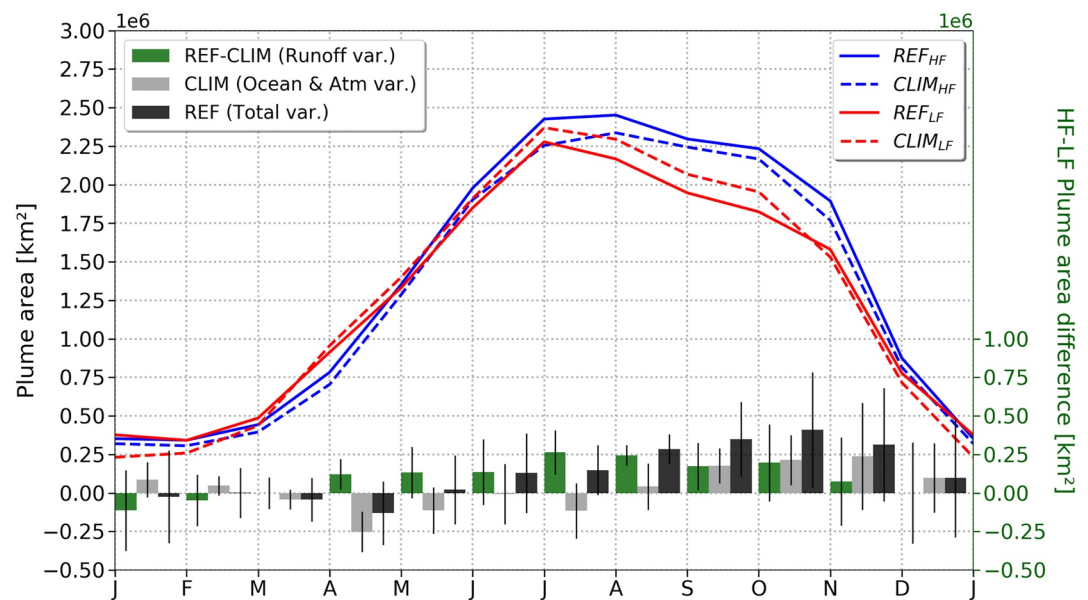


Figure 6. Seasonal cycle of the plume extent of each composite (curves), and of the differences between composites with their errors (bar chart).

large, but the values are significant nonetheless. This means that the effect of the extreme floods on the salinity budget may be smaller in some years, but is consistently detectable.

3.2. Impact of Runoff Interannual Variability on the Plume Area

Another relevant and commonly studied feature is the plume extent, whose seasonal cycle is shown in Figure 6 for the two simulations, for the lowest and highest floods years. The plume extent is at its lowest in winter, increases during spring and reaches its highest values in summer and fall. This is consistent with Coles et al. (2013), but not exactly with Moller et al. (2010), who found smaller values of plume extent, and a seasonal cycle peaking in July and decreasing shortly after. However, Moller et al. (2010) used a different threshold value for the plume (34 instead of 35 PSU) and their area of analysis is smaller. We obtain a comparable seasonal cycle by using the same criterion as them (not shown).

The impact of the runoff interannual variability on the plume extent is also substantial. During the season of largest plume extent, that is August-September-October (ASO), the total change in plume extent (i.e., the difference between REF composites, Figure 6, black bars) is around 16%. Around three quarters of this change is explained by runoff interannual variability (i.e., the difference between REF and CLIM composites, Figure 6, gray bars). This is in perfect agreement with Moller et al. (2010), who found that runoff interannual variability explained 74% of the plume extent variability. This is also in agreement with Zeng et al. (2008), who did not quantify the impact of runoff variability on the plume extent, but found a strong correlation between Amazon runoff and plume extent interannual anomalies.

3.3. Impact of Runoff Interannual Variability on SST

As done for the SSS, we isolate the effect of the runoff interannual variability on the SST (Figures 7a and 7b) from the changes due to the other forcings (Figures 7c and 7d). Despite a strong impact on SSS (Figure 4c), the runoff interannual variability leads to very weak changes in SST in spring (Figure 7a). More importantly, these changes are negligible compared to the strong changes in SST induced by ocean and atmospheric variability (Figure 7c), which can most likely be related to the AMM (see Section 4.1). During an AMM event, the SST anomalies associated with this event tend to disappear from July onwards (e.g., Foltz et al., 2012). This explains the weakening of the SST anomalies due to ocean and atmospheric variability observed in summer (Figure 7d): the negative anomaly decreases from -0.5°C in spring to -0.1°C in summer (average on 0° – 20°N , 80° – 20°W).

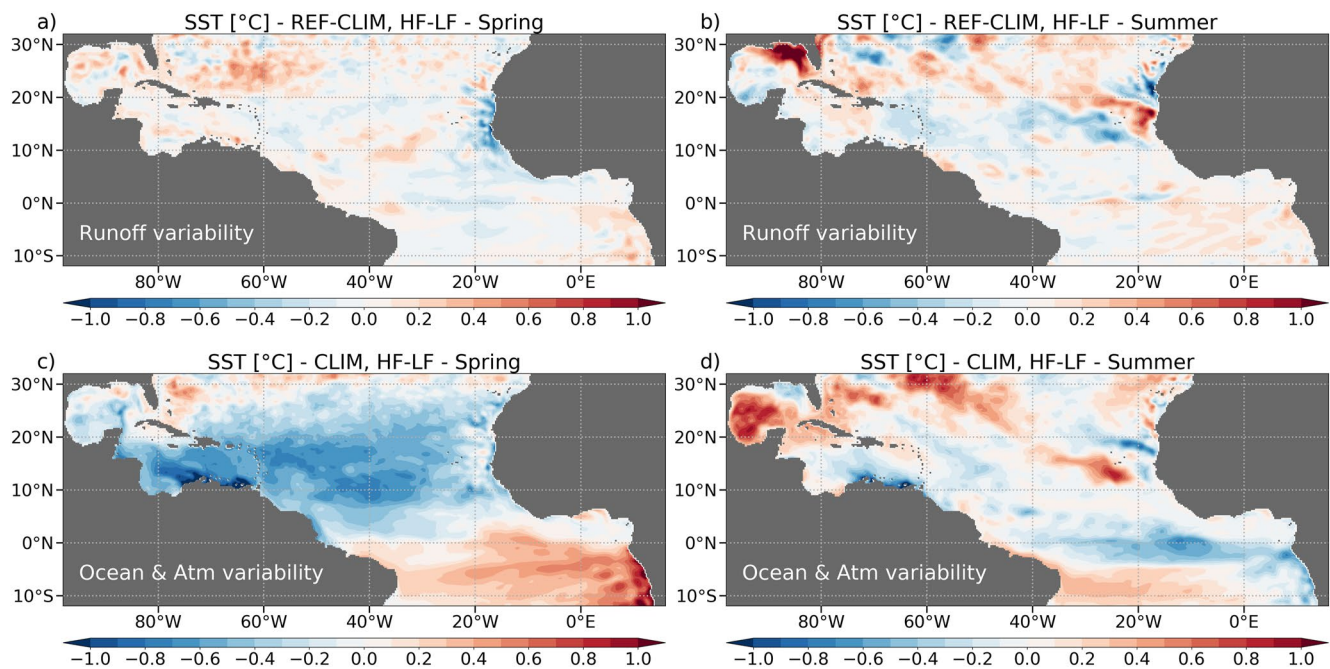


Figure 7. Spring (April-May-June) maps of SST differences between highest floods and lowest floods for (a) CLIM and (c) REF minus CLIM; (b and d): same as (a and c) respectively but in summer (July-August-September).

The impact of interannual runoff variability remains weak (Figure 7b), which was expected since the salinity anomaly is already fading in summer (Figure 4d).

4. Discussion

4.1. Influence of the Atlantic Meridional Mode

A large part of the variability captured by the chosen composites is likely caused by the AMM. First of all, runoff interannual variability can be linked to AMM. The 2009 Amazon flood has been directly related to a negative AMM event (Foltz et al., 2012). Moreover, several Amazon droughts occurred during warm events in the North tropical Atlantic, characteristic of positive AMM phases, while several Amazon floods occurred during warm events in the South tropical Atlantic, characteristic of negative AMM phases (e.g., Marengo & Espinoza, 2016). The difference between highest floods and lowest floods composites can therefore be associated with a negative AMM phase. And indeed, some patterns that emerge are very characteristic of a negative AMM event, as described below.

AMM is primarily characterized by a dipole of SST anomalies, which peaks in spring. For a negative AMM event, the SST anomalies are negative in the northern hemisphere, and positive in the southern hemisphere. This pattern is identical to what is observed in spring in the map of SST difference between the REF composites (not shown, but very similar to Figure 7c). This is also consistent with results from Fournier et al. (2017), who found strong negative SST anomalies in 2014 (one of the years composing our highest floods composite), and strong positive anomalies in 2010 (one of the years composing our lowest floods composite).

The SST dipole generates a southward shift of the ITCZ during negative AMM phase, and therefore an increase in precipitation over the Amazon basin (Grodky et al., 2018; Rugg et al., 2016; Xie & Carton, 2004), leading to higher Amazon floods in the process. This ITCZ shift is clearly observed in the map of precipitation difference between the REF composites (Figure 8), and it is similar to what Jury (2019) observed when doing a difference between fresh and salty years.

The SSS signature of AMM has been extracted by Awo et al. (2018), and is similar to what is obtained here (Figure 4a). Moreover, the changes in currents previously identified as drivers of SSS variability are likely caused

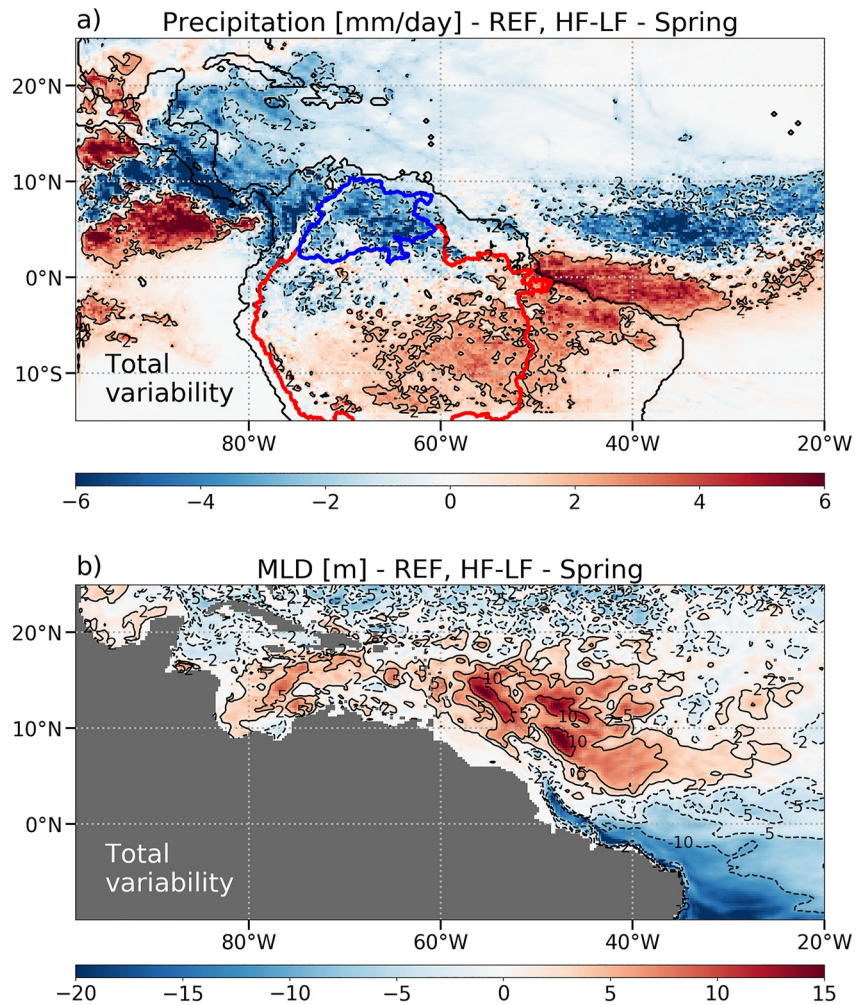


Figure 8. Map of (a) precipitation and (b) mixed layer depth in spring (April-May-June), difference between the REF composites. The contours of the Orinoco (in blue) and Amazon (in red) watersheds are represented on (a).

by the AMM, especially the southward shift of NECC in spring (Hormann et al., 2012), the increase in NBC and the decrease in NBC retroflection in summer (Jury, 2019).

Finally, it is interesting to note that the MLD is also strongly impacted by the AMM: during negative AMM events, a deepening of the ML is observed in the northwestern part of the basin (including the Amazon plume), despite the strong SSS decrease and the increase in salinity stratification induced by Amazon extreme floods (Rugg et al., 2016, see also Figure 8). This shows that the Amazon extreme floods do not have a strong impact on the vertical dynamics in the Amazon plume. This ML deepening is most likely related to a wind increase (not shown, see Rugg et al., 2016), but also to the SST decrease previously discussed, which suggests that temperature changes linked to AMM have a stronger control on stratification than salinity changes due to extreme floods.

4.2. SSS Changes in the Orinoco Plume

A strong positive anomaly (62°W, 10°N) can be observed in Figure 4b, which corresponds to the location of the Orinoco river mouth. Indeed, the variability of the Orinoco discharge is generally opposite to that of the Amazon. First, the monthly Amazon and Orinoco discharge are anticorrelated, albeit weakly ($R = -0.30$ with a 3-month lag). Moreover, this opposite variability is very noticeable during extreme flood events: years of low floods of the Amazon (2003, 2004, 2007, 2010) correspond to years of high floods for the Orinoco, and some of the major Amazon floods (2009, 2014) coincide with years of low floods for the Orinoco (see Figures 2a and 2b). This is

driven by ITCZ interannual variability. Indeed, Amazon floods usually occur when the ITCZ is anomalously far south. This ITCZ shift, usually due to a negative AMM phase, then leads to a lack of precipitation in the north of the Amazon watershed and in the Orinoco watershed (see Figure 8a). One can also note that the effect of the Orinoco is not observed in spring (Figure 4a) but only in summer (Figure 4b). This is due to the fact that summer is the time of year when the Orinoco discharge is the highest (Müller-Karger et al., 1989) and has the largest effect on SSS.

Nevertheless, this process is not sufficient to explain the whole response near the Orinoco mouth: Figure 4f shows that ocean and atmospheric processes also are important.

5. Summary

In this study, we used a coupled ocean-atmosphere model at a $1/4^\circ$ resolution to assess the impact of runoff interannual variability on SSS, plume extent and SST in the western tropical Atlantic. The focus is on the flood season (viz. boreal spring-summer). The use of a coupled ocean-atmosphere model is motivated by the fact that the ocean-atmosphere feedback loop must be modeled in order to properly investigate the impacts of the plume on the SST, in particular to release the constraint that would be exerted on the SST, in a context of forced ocean modeling, by prescribed and non-interactive atmospheric forcings. Two 15-years experiments are conducted: a REF experiment with interannual variability of river runoff and ocean color, and a CLIM experiment forced with 2001–2015 monthly climatologies of runoff and ocean color. To investigate the effect of the extreme floods observed in recent decades, we calculated composites of the 4 years with the highest floods and the 4 years with the lowest floods. The runoff change between highest and lowest floods years is about 25%. Finally, we calculated differences of the two composites, for the REF and CLIM experiment as well as for the REF minus CLIM difference. This allowed us to isolate the effect of runoff interannual variability from other ocean and atmospheric processes (mixing, advection, atmospheric water and heat fluxes) whose variability can impact the salinity and temperature properties of the western tropical Atlantic.

Runoff interannual variability has a strong impact on the SSS of the Amazon plume in spring (freshening of more than 3 PSU near the Amazon mouth). However, this effect fades rapidly under the action of vertical mixing, and has completely disappeared by fall. Such a rapid damping of salinity anomalies by vertical mixing has already been observed in other tropical river plumes, such as the Ganges and Brahmaputra plume in the Bay of Bengal (Benshila et al., 2014). The ocean and atmospheric variability impacts the SSS to a similar magnitude as runoff. In spring, a decrease in NBC and in coastal currents leads to an accumulation of freshwater near the Amazon mouth and a salty anomaly downstream, near the Guiana coast. In summer, a decrease in NBC retroflection leads to a stronger northwestward freshwater transport into the Lesser Antilles, and less freshwater transport into the NECC. These currents changes can be associated with AMM.

The plume area is also affected by extreme floods in summer and fall, the period when it is the most extended. In ASO, a change of 16% in plume area is observed, and runoff interannual variability explains 75% of it.

Finally, we show that years with high and low floods are associated with strong SST anomalies in spring in the north tropical Atlantic. This anomaly is linked with a negative phase of the AMM and therefore a southward shift of the ITCZ, which in turn causes Amazon floods. Some of these extreme floods events could also be exacerbated by ENSO events: moderate to strong El Niño events occurred in 2003 and 2010, two of the years included in our lowest floods composite, and a strong La Niña event occurred in 2008, a year included in our highest floods composite. But our simulations do not reveal any clear impact of the runoff interannual variability on the SST, neither in spring nor in summer.

At first glance, these results may seem contradictory with some of the previous observational studies. Indeed, it has been previously suggested that currents were the main driver of SSS interannual variability, with very weak impact of the runoff (Fournier et al., 2017; Grodsky et al., 2014, 2015). However, these observational studies are usually located relatively far from the Amazon mouth and from the core of the Amazon plume: for instance, Grodsky et al. (2015) studied the Antilles, while Fournier et al. (2017) study is focused on the northern part of the plume (NPR), between 51°W and 59°W and between 13°N and 22°N . Another issue can be the period studied: Fournier et al. (2017) focused for instance on the month of August, whereas we saw in this study that the response to anomalous floods is short-lived, and has almost disappeared at this time of the year.

The hydrological cycle is currently intensifying, in particular in the Amazon basin (Barichivich et al., 2018; Espinoza, Guyot, et al., 2009; Gloor et al., 2013; Marengo & Espinoza, 2016). A new record flood affected the region in 2021 and, including it, it turns out that 7 of the 10 largest Amazon floods have occurred in the last 13 years (Chevuturi et al., 2021). This trend is expected to intensify further under the influence of climate change (Allan et al., 2020; Skliris et al., 2016). Moreover, the Amazon basin is currently subject to profound anthropogenic changes that also alter the hydrological cycle (e.g., Latrubesse et al., 2017). Deforestation for instance has been shown to decrease evapotranspiration and increase runoff, and to a lesser extent increase extreme events intensity (Coe et al., 2009; Guimberteau et al., 2017). The construction of numerous dams in the Amazon watershed (Anderson et al., 2018) could on the other hand mitigate floods frequency and strength (Boulangé et al., 2021), despite strong impacts on the hydrological cycle, ecosystems and fisheries (e.g., Santos et al., 2018; Timpe & Kaplan, 2017). This land-use planning is bound to continue, as is climate change, unless a radical shift in environmental policies occurs. It would therefore be worth revisiting these results in the near future.

Data Availability Statement

The coupled ocean-atmosphere configuration is available here: <https://doi.org/10.5281/zenodo.6448250> (Gévaudan et al., 2022). Sea surface salinity data set from ESA Climate Change Initiative project is freely available at <https://www.doi.org/10.5285/4ce685bff631459fb2a30faa699f3fc5> (Boutin et al., 2020). Chlorophyll data set from GlobColour (009_082) can be obtained at <https://www.doi.org/10.48670/moi-00100>.

Acknowledgments

This study received support from ESA CCI+SSS and TOSCA SSS projects. Computing facilities were provided by GENCI (project GEN7298).

References

- Allan, R., Barlow, M., Byrne, M. P., Cherchi, A., Douville, H., Fowler, H. J., et al. (2020). Advances in understanding large-scale responses of the water cycle to climate change. *Annals of the New York Academy of Sciences*, 1472(1), 49–75. <https://doi.org/10.1111/nyas.14337>
- Alory, G., Delcroix, T., Téchiné, P., Diverrès, D., Varillon, D., Cravatte, S., et al. (2015). The French contribution to the voluntary observing ships network of sea surface salinity. *Deep Sea Research Part I: Oceanographic Research Papers*, 105, 1–18. <https://doi.org/10.1016/j.dsr.2015.08.005>
- Anderson, E. P., Jenkins, C. N., Heilpern, S., Maldonado-Ocampo, J. A., Carvajal-Vallejos, F. M., Encalada, A. C., et al. (2018). Fragmentation of Andes-to-Amazon connectivity by hydropower dams. *Science Advances*, 4(1). <https://doi.org/10.1126/sciadv.aao1642>
- Awo, F. M., Alory, G., Da-Allada, C. Y., Delcroix, T., Jouanno, J., Kestenare, E., & Baloitcha, E. (2018). Sea surface salinity signature of the tropical Atlantic interannual climatic modes. *Journal of Geophysical Research: Oceans*, 123(10), 7420–7437. <https://doi.org/10.1029/2018jc013837>
- Balaguru, K., Chang, P., Saravanan, R., & Jang, C. J. (2012). The barrier layer of the Atlantic warmpool: Formation mechanism and influence on the mean climate. *Tellus A: Dynamic Meteorology and Oceanography*, 64(1), 18162. <https://doi.org/10.3402/tellusa.v64i0.18162>
- Balaguru, K., Foltz, G. R., Leung, L. R., Kaplan, J., Xu, W., Reul, N., & Chapron, B. (2020). Pronounced impact of salinity on rapidly intensifying tropical cyclones. *Bulletin of the American Meteorological Society*, 101(9), E1497–E1511. <https://doi.org/10.1175/BAMS-D-19-0303.1>
- Barichivich, J., Gloor, E., Peylin, P., Brienen, R. J., Schöngart, J., Espinoza, J. C., & Pattayak, K. C. (2018). Recent intensification of Amazon flooding extremes driven by strengthened Walker circulation. *Science Advances*, 4(9). <https://doi.org/10.1126/sciadv.aat8785>
- Benshila, R., Durand, F., Masson, S., Bourdallé-Badie, R., deBoyer Montégut, C., Papa, F., & Madec, G. (2014). The upper Bay of Bengal salinity structure in a high-resolution model. *Ocean Modelling*, 74, 36–52. <https://doi.org/10.1016/j.ocemod.2013.12.001>
- Boulangé, J., Hanasaki, N., Yamazaki, D., & Pokhrel, Y. (2021). Role of dams in reducing global flood exposure under climate change. *Nature Communications*, 12(1), 417. <https://doi.org/10.1038/s41467-020-20704-0>
- Boutin, J., Vergely, J.-L., Marchand, S., d'Amico, F., Hasson, A., Kolodziejczyk, N., et al. (2018). New SMOS sea surface salinity with reduced systematic errors and improved variability. *Remote Sensing of Environment*, 214, 115–134. <https://doi.org/10.1016/j.rse.2018.05.022>
- Boutin, J., Vergely, J.-L., Reul, N., Catany, R., Koehler, J., Martin, A., et al. (2020). *ESA Sea Surface Salinity Climate Change Initiative: Weekly and monthly sea surface salinity products, v2.31, for 2010 to 2019*. Centre for Environmental Data Analysis. <https://doi.org/10.5285/4ce685bff631459fb2a30faa699f3fc5>
- Camara, I., Kolodziejczyk, N., Mignot, J., Lazar, A., & Gaye, A. T. (2015). On the seasonal variations of salinity of the tropical Atlantic mixed layer. *Journal of Geophysical Research: Oceans*, 120(6), 4441–4462. <https://doi.org/10.1002/2015JC010865>
- Chevuturi, A., Klingaman, N. P., Rudorff, C. M., Coelho, C. A. S., & Schöngart, J. (2021). Forecasting annual maximum water level for the Negro River at Manaus. *Climate Resilience and Sustainability*, 1(1), e18. <https://doi.org/10.1002/cli.18>
- Coe, M. T., Costa, M. H., & Soares-Filho, B. S. (2009). The influence of historical and potential future deforestation on the stream flow of the Amazon River—Land surface processes and atmospheric feedbacks. *Journal of Hydrology*, 369(1–2), 165–174. <https://doi.org/10.1016/j.jhydrol.2009.02.043>
- Coles, V. J., Brooks, M. T., Hopkins, J., Stukel, M. R., Yager, P. L., & Hood, R. R. (2013). The pathways and properties of the Amazon river plume in the tropical North Atlantic Ocean. *Journal of Geophysical Research: Oceans*, 118(12), 6894–6913. <https://doi.org/10.1002/2013JC008981>
- Craig, A., Valcke, S., & Coquart, L. (2017). Development and performance of a new version of the OASIS coupler, OASIS3-MCT_3.0. *Geoscientific Model Development*, 10(9), 3297–3308. <https://doi.org/10.5194/gmd-10-3297-2017>
- de Boyer Montégut, C., Vialard, J., Shenoi, S. S. C., Shankar, D., Durand, F., Ethé, C., & Madec, G. (2007). Simulated seasonal and interannual variability of the mixed layer heat budget in the Northern Indian Ocean. *Journal of Climate*, 20(13), 3249–3268. <https://doi.org/10.1175/JCLI4148.1>
- Decharme, B., Delire, C., Minvielle, M., Colin, J., Vergnes, J.-P., Alias, A., et al. (2019). Recent changes in the ISBA-CTrip land surface system for use in the CNRM-CM6 climate model and in global off-line hydrological applications. *Journal of Advances in Modeling Earth Systems*, 11(5), 1207–1252. <https://doi.org/10.1029/2018MS001545>

- Dee, D. P., Uppala, S. M., Simmons, A., Berrisford, P., Poli, P., Kobayashi, S., et al. (2011). The ERA-Interim reanalysis: Configuration and performance of the data assimilation system. *Quarterly Journal of the Royal Meteorological Society*, *137*(656), 553–597. <https://doi.org/10.1002/qj.828>
- Delcroix, T., Alory, G., T  chin  , P., Diverr  s, D., Varillon, D., Cravatte, S., et al. (2002). Sea surface salinity data from voluntary observing ships network. *Odatis*. <https://doi.org/10.6096/SSS-LEGOS>
- Drumond, A., Marengo, J., Ambrizzi, T., Nieto, R., Moreira, L., & Gimeno, L. (2014). The role of the Amazon basin moisture in the atmospheric branch of the hydrological cycle: A Lagrangian analysis. *Hydrology and Earth System Sciences*, *18*(7), 2577–2598. <https://doi.org/10.5194/hess-18-2577-2014>
- Dussin, R., Barnier, B., Brodeau, L., & Molines, J. (2016). *The making of the Drakkar forcing set DFS5 01-04*. DRAKKAR/MyOcean Rep.
- Espinoza, J. C., Guyot, J. L., Ronchail, J., Cochonneau, G., Filizola, N., Fraizy, P., et al. (2009). Contrasting regional discharge evolutions in the Amazon basin (1974–2004). *Journal of Hydrology*, *375*(3–4), 297–311. <https://doi.org/10.1016/j.jhydrol.2009.03.004>
- Espinoza, J. C., Ronchail, J., Guyot, J. L., Cochonneau, G., Naziano, F., Lavado, W., et al. (2009). Spatio-temporal rainfall variability in the Amazon basin countries (Brazil, Peru, Bolivia, Colombia, and Ecuador). *International Journal of Climatology: A Journal of the Royal Meteorological Society*, *29*(11), 1574–1594. <https://doi.org/10.1002/joc.1791>
- Espinoza, J. C., Segura, H., Ronchail, J., Drapeau, G., & Gutierrez-Cori, O. (2016). Evolution of wet-day and dry-day frequency in the western Amazon basin: Relationship with atmospheric circulation and impacts on vegetation. *Water Resources Research*, *52*(11), 8546–8560. <https://doi.org/10.1002/2016WR019305>
- Fassoni-Andrade, A. C., Fleischmann, A. S., Papa, F., de Paiva, R. C. D., Wongchuig, S., Melack, J. M., et al. (2021). Amazon hydrology from space: Scientific advances and future challenges. *Reviews of Geophysics*, *59*(4), e2020RG000728. <https://doi.org/10.1029/2020rg000728>
- Ferry, N., Parent, L., Garric, G., Bricaud, C., Testut, C., Le Galloudec, O., et al. (2012). GLORYS2V1 global ocean reanalysis of the altimetric era (1992–2009) at mesoscale. *Mercator Ocean-Quarterly Newsletter*, *44*.
- Ferry, N., & Reverdin, G. (2004). Sea surface salinity interannual variability in the western tropical Atlantic: An ocean general circulation model study. *Journal of Geophysical Research*, *109*(C5), C05026. <https://doi.org/10.1029/2003JC002122>
- Ffield, A. (2007). Amazon and Orinoco river plumes and NBC rings: Bystanders or participants in hurricane events? *Journal of Climate*, *20*(2), 316–333. <https://doi.org/10.1175/JCLI3985.1>
- Filizola, N., Latrubesse, E. M., Fraizy, P., Souza, R., Guimar  es, V., & Guyot, J.-L. (2014). Was the 2009 flood the most hazardous or the largest ever recorded in the Amazon? *Geomorphology*, *215*, 99–105. <https://doi.org/10.1016/j.geomorph.2013.05.028>
- Foltz, G. R., Grodsky, S. A., Carton, J. A., & McPhaden, M. J. (2004). Seasonal salt budget of the northwestern tropical Atlantic Ocean along 38  W. *Journal of Geophysical Research*, *109*(C3). <https://doi.org/10.1029/2003JC002111>
- Foltz, G. R., McPhaden, M. J., & Lumpkin, R. (2012). A strong Atlantic meridional mode event in 2009: The role of mixed layer dynamics. *Journal of Climate*, *25*(1), 363–380. <https://doi.org/10.1175/JCLI-D-11-00150.1>
- Fournier, S., Vandemark, D., Gaultier, L., Lee, T., Jonsson, B., & Gierach, M. M. (2017). Interannual variation in offshore advection of Amazon-Orinoco plume waters: Observations, forcing mechanisms, and impacts. *Journal of Geophysical Research: Oceans*, *122*(11), 8966–8982. <https://doi.org/10.1002/2017JC013103>
- Friedman, A. R., Bollasina, M. A., Gastineau, G., & Khodri, M. (2021). Increased Amazon Basin wet-season precipitation and river discharge since the early 1990s driven by tropical Pacific variability. *Environmental Research Letters*, *16*(3), 034033. <https://doi.org/10.1088/1748-9326/abd587>
- Garnesson, P., Mangin, A., d'Andon, O. F., Demaria, J., & Bretagnon, M. (2019). The CMEMS GlobColour chlorophyll *a* product based on satellite observation: Multi-sensor merging and flagging strategies. *Ocean Science*, *15*(3), 819–830. <https://doi.org/10.5194/os-15-819-2019>
- G  vaudan, M., Jouanno, J., & Durand, F. (2022). A NEMO-OASIS-WRF coupled configuration of the tropical Atlantic Ocean. *Zenodo*. <https://doi.org/10.5281/zenodo.6448250>
- G  vaudan, M., Jouanno, J., Durand, F., Morvan, G., Renault, L., & Samson, G. (2021). Influence of ocean salinity stratification on the tropical Atlantic Ocean surface. *Climate Dynamics*, *57*(1–2), 321–340. <https://doi.org/10.1007/s00382-021-05713-z>
- Giffard, P., Llovel, W., Jouanno, J., Morvan, G., & Decharme, B. (2019). Contribution of the Amazon river discharge to regional sea level in the tropical Atlantic Ocean. *Water*, *11*(11), 2348. <https://doi.org/10.3390/w11112348>
- Gloor, M., Barichivich, J., Ziv, G., Brienen, R., Sch  ngart, J., Peylin, P., et al. (2015). Recent Amazon climate as background for possible ongoing and future changes of Amazon humid forests. *Global Biogeochemical Cycles*, *29*(9), 1384–1399. <https://doi.org/10.1002/2014GB005080>
- Gloor, M., Brienen, R. J., Galbraith, D., Feldpausch, T. R., Sch  ngart, J., Guyot, J.-L., et al. (2013). Intensification of the Amazon hydrological cycle over the last two decades. *Geophysical Research Letters*, *40*(9), 1729–1733. <https://doi.org/10.1002/grl.50377>
- Gouveia, N., Gherardi, D., & Arag  o, L. (2019). The role of the Amazon river plume on the intensification of the hydrological cycle. *Geophysical Research Letters*, *46*(21), 12221–12229. <https://doi.org/10.1029/2019GL084302>
- Grodsky, S. A., Johnson, B. K., Carton, J. A., & Bryan, F. O. (2015). Interannual Caribbean salinity in satellite data and model simulations. *Journal of Geophysical Research: Oceans*, *120*(2), 1375–1387. <https://doi.org/10.1002/2014JC010625>
- Grodsky, S. A., Reverdin, G., Carton, J. A., & Coles, V. J. (2014). Year-to-year salinity changes in the Amazon plume: Contrasting 2011 and 2012 Aquarius/SACD and SMOS satellite data. *Remote Sensing of Environment*, *140*, 14–22. <https://doi.org/10.1016/j.rse.2013.08.033>
- Grodsky, S. A., Vandemark, D., & Feng, H. (2018). Assessing coastal SMAP surface salinity accuracy and its application to monitoring Gulf of Maine circulation dynamics. *Remote Sensing*, *10*(8), 1232. <https://doi.org/10.3390/rs10081232>
- Guimberteau, M., Ciais, P., Ducharne, A., Boisier, J. P., Aguiar, A. P. D., Biemans, H., et al. (2017). Impacts of future deforestation and climate change on the hydrology of the Amazon basin: A multi-model analysis with a new set of land-cover change scenarios. *Hydrology and Earth System Sciences*, *21*(3), 1455–1475. <https://doi.org/10.5194/hess-21-1455-2017>
- Hellweger, F. L., & Gordon, A. L. (2002). Tracing Amazon River water into the Caribbean Sea. *Journal of Marine Research*, *60*(4), 537–549. <https://doi.org/10.1357/002224002762324202>
- Hernandez, O., Jouanno, J., & Durand, F. (2016). Do the Amazon and Orinoco freshwater plumes really matter for hurricane-induced ocean surface cooling? *Journal of Geophysical Research: Oceans*, *121*(4), 2119–2141. <https://doi.org/10.1002/2015JC011021>
- Hernandez, O., Jouanno, J., Echevin, V., & Aumont, O. (2017). Modification of sea surface temperature by chlorophyll concentration in the Atlantic upwelling systems. *Journal of Geophysical Research: Oceans*, *122*(7), 5367–5389. <https://doi.org/10.1002/2016JC012330>
- Hormann, V., Lumpkin, R., & Foltz, G. R. (2012). Interannual North Equatorial Countercurrent variability and its relation to tropical Atlantic climate modes. *Journal of Geophysical Research*, *117*(C4), C04035. <https://doi.org/10.1029/2011JC007697>
- Huang, B., & Mehta, V. M. (2010). Influences of freshwater from major rivers on global ocean circulation and temperatures in the MIT ocean general circulation model. *Advances in Atmospheric Sciences*, *27*(3), 455–468. <https://doi.org/10.1007/s00376-009-9022-6>
- Jahfer, S., Vinayachandran, P., & Nanjundiah, R. S. (2017). Long-term impact of Amazon river runoff on northern hemispheric climate. *Scientific Reports*, *7*(1), 1–9. <https://doi.org/10.1038/s41598-017-10750-y>

- Jahfer, S., Vinayachandran, P., & Nanjundiah, R. S. (2020). The role of Amazon river runoff on the multidecadal variability of the Atlantic ITCZ. *Environmental Research Letters*, *15*(5), 054013. <https://doi.org/10.1088/1748-9326/ab7c8a>
- Jury, M. R. (2019). Factors underlying changes in salinity around the southeastern Antilles. *Journal of Marine Systems*, *199*, 103208. <https://doi.org/10.1016/j.jmarsys.2019.103208>
- Large, W. G., & Yeager, S. G. (2009). The global climatology of an interannually varying air-sea flux data set. *Climate Dynamics*, *33*(2–3), 341–364. <https://doi.org/10.1007/s00382-008-0441-3>
- Latrubesse, E. M., Arima, E. Y., Dunne, T., Park, E., Baker, V. R., d'Horta, F. M., et al. (2017). Damming the rivers of the Amazon basin. *Nature*, *546*(7658), 363–369. <https://doi.org/10.1038/nature22333>
- Li, X., Xie, S.-P., Gille, S. T., & Yoo, C. (2016). Atlantic-induced pan-tropical climate change over the past three decades. *Nature Climate Change*, *6*(3), 275–279. <https://doi.org/10.1038/nclimate2840>
- Liang, Y.-C., Lo, M.-H., Lan, C.-W., Seo, H., Ummenhofer, C. C., Yeager, S., et al. (2020). Amplified seasonal cycle in hydroclimate over the Amazon river basin and its plume region. *Nature Communications*, *11*(1), 1–11. <https://doi.org/10.1038/s41467-020-18187-0>
- Locarnini, M., Mishonov, A., Baranova, O., Boyer, T., Zweng, M., Garcia, H., et al. (2018). World Ocean Atlas volume 1.
- Madec, G., & the NEMO team (2016). NEMO ocean engine. *Note du Pôle de modélisation* (Vol. 27, pp. 1288–1619). Institut Pierre-Simon Laplace (IPSL).
- Marengo, J. A., Borma, L. S., Rodríguez, D. A., Pinho, P., Soares, W. R., & Alves, L. M. (2013). Recent extremes of drought and flooding in Amazonia: Vulnerabilities and human adaptation. *American Journal of Climate Change*, *02*(02), 87–96. <https://doi.org/10.4236/ajcc.2013.22009>
- Marengo, J. A., & Espinoza, J. C. (2016). Extreme seasonal droughts and floods in Amazonia: Causes, trends and impacts. *International Journal of Climatology*, *36*(3), 1033–1050. <https://doi.org/10.1002/joc.4420>
- Marengo, J. A., Nobre, C. A., Tomasella, J., Oyama, M. D., Sampaio de Oliveira, G., De Oliveira, R., et al. (2008). The drought of Amazonia in 2005. *Journal of Climate*, *21*(3), 495–516. <https://doi.org/10.1175/2007JCLI1600.1>
- Marengo, J. A., Tomasella, J., Alves, L. M., Soares, W. R., & Rodríguez, D. A. (2011). The drought of 2010 in the context of historical droughts in the Amazon region. *Geophysical Research Letters*, *38*(12), L12703. <https://doi.org/10.1029/2011GL047436>
- Maritorena, S., d'Andon, O. H. F., Mangin, A., & Siegel, D. A. (2010). Merged satellite ocean color data products using a bio-optical model: Characteristics, benefits and issues. *Remote Sensing of Environment*, *114*(8), 1791–1804. <https://doi.org/10.1016/j.rse.2010.04.002>
- Masson, S., & Delecluse, P. (2001). Influence of the Amazon river runoff on the tropical Atlantic. *Physics and Chemistry of the Earth - Part B: Hydrology, Oceans and Atmosphere*, *26*(2), 137–142. [https://doi.org/10.1016/S1464-1909\(00\)00230-6](https://doi.org/10.1016/S1464-1909(00)00230-6)
- McGregor, S., Timmermann, A., Stuecker, M. F., England, M. H., Merrifield, M., Jin, F.-F., & Chikamoto, Y. (2014). Recent Walker circulation strengthening and Pacific cooling amplified by Atlantic warming. *Nature Climate Change*, *4*(10), 888–892. <https://doi.org/10.1038/nclimate2330>
- Molleri, G. S., Novo, E. M. d. M., & Kampel, M. (2010). Space-time variability of the Amazon River plume based on satellite ocean color. *Continental Shelf Research*, *30*(3–4), 342–352. <https://doi.org/10.1016/j.csr.2009.11.015>
- Morel, A., & Bérthon, J.-F. (1989). Surface pigments, algal biomass profiles, and potential production of the euphotic layer: Relationships investigated in view of remote-sensing applications. *Limnology & Oceanography*, *34*(8), 1545–1562. <https://doi.org/10.4319/lo.1989.34.8.1545>
- Müller-Karger, F., McClain, C., Fisher, T., Esaias, W., & Varela, R. (1989). Pigment distribution in the Caribbean sea: Observations from space. *Progress in Oceanography*, *23*(1), 23–64. [https://doi.org/10.1016/0079-6611\(89\)90024-4](https://doi.org/10.1016/0079-6611(89)90024-4)
- Newinger, C., & Toumi, R. (2015). Potential impact of the colored Amazon and Orinoco plume on tropical cyclone intensity. *Journal of Geophysical Research: Oceans*, *120*(2), 1296–1317. <https://doi.org/10.1002/2014JC010533>
- Pailler, K., Bourlès, B., & Gouriou, Y. (1999). The barrier layer in the western tropical Atlantic Ocean. *Geophysical Research Letters*, *26*(14), 2069–2072. <https://doi.org/10.1029/1999GL900492>
- Reeves Eyre, J. J., & Zeng, X. (2021). The Amazon water cycle: Perspectives from water budget closure and ocean salinity. *Journal of Climate*, *34*(4), 1439–1451. <https://doi.org/10.1175/JCLI-D-20-0309.1>
- Reul, N., Grodsky, S., Arias, M., Boutin, J., Catany, R., Chapron, B., et al. (2020). Sea surface salinity estimates from spaceborne L-band radiometers: An overview of the first decade of observation (2010–2019). *Remote Sensing of Environment*, *242*, 111769. <https://doi.org/10.1016/j.rse.2020.111769>
- Ronchail, J., Labat, D., Callède, J., Cochonneau, G., Guyot, J.-L., Filizola, N., & de Oliveira, E. (2005). Discharge variability within the Amazon basin. In *Regional hydrological impacts of climatic change-hydroclimatological variability (proceedings of symposium s6 held during the seventh iahs scientific assembly at foz do iguaçu, Brazil)*.
- Ropelewski, C. F., & Halpert, M. S. (1987). Global and regional scale precipitation patterns associated with the El Niño/Southern Oscillation. *Monthly Weather Review*, *115*(8), 1606–1626. [https://doi.org/10.1175/1520-0493\(1987\)115<1606:garspp>2.0.co;2](https://doi.org/10.1175/1520-0493(1987)115<1606:garspp>2.0.co;2)
- Ruault, V., Jouanno, J., Durand, F., Chanut, J., & Benshila, R. (2020). Role of the tide on the structure of the Amazon plume: A numerical modeling approach. *Journal of Geophysical Research: Oceans*, *125*(2), e2019JC015495. <https://doi.org/10.1029/2019JC015495>
- Rugg, A., Foltz, G. R., & Perez, R. C. (2016). Role of mixed layer dynamics in tropical North Atlantic interannual sea surface temperature variability. *Journal of Climate*, *29*(22), 8083–8101. <https://doi.org/10.1175/JCLI-D-15-0867.1>
- Salisbury, J., Vandemark, D., Campbell, J., Hunt, C., Wissler, D., Reul, N., & Chapron, B. (2011). Spatial and temporal coherence between Amazon River discharge, salinity, and light absorption by colored organic carbon in western tropical Atlantic surface waters. *Journal of Geophysical Research*, *116*(C7), 2011JC006989. <https://doi.org/10.1029/2011JC006989>
- Santos, R. E., Pinto-Coelho, R. M., Fonseca, R., Simões, N. R., & Zanchi, F. B. (2018). The decline of fisheries on the Madeira River, Brazil: The high cost of the hydroelectric dams in the Amazon Basin. *Fisheries Management and Ecology*, *25*(5), 380–391. <https://doi.org/10.1111/fme.12305>
- Skamarock, W. C., & Klemp, J. B. (2008). A time-split nonhydrostatic atmospheric model for weather research and forecasting applications. *Journal of Computational Physics*, *227*(7), 3465–3485. <https://doi.org/10.1016/j.jcp.2007.01.037>
- Skirris, N., Zika, J. D., Nurser, G., Josey, S. A., & Marsh, R. (2016). Global water cycle amplifying at less than the Clausius-Clapeyron rate. *Scientific Reports*, *6*(1), 1–9. <https://doi.org/10.1038/srep38752>
- Timpe, K., & Kaplan, D. (2017). The changing hydrology of a dammed Amazon. *Science Advances*, *3*(11). <https://doi.org/10.1126/sciadv.1700611>
- Towner, J., Cloke, H. L., Lavado, W., Santini, W., Bazo, J., Coughlan de Perez, E., & Stephens, E. M. (2020). Attribution of Amazon floods to modes of climate variability: A review. *Meteorological Applications*, *27*(5), e1949. <https://doi.org/10.1002/met.1949>
- Varona, H., Veleda, D., Silva, M., Cintra, M., & Araujo, M. (2019). Amazon River plume influence on Western Tropical Atlantic dynamic variability. *Dynamics of Atmospheres and Oceans*, *85*, 1–15. <https://doi.org/10.1016/j.dynatmoce.2018.10.002>
- Wang, X.-Y., Li, X., Zhu, J., & Tanajura, C. A. (2018). The strengthening of Amazonian precipitation during the wet season driven by tropical sea surface temperature forcing. *Environmental Research Letters*, *13*(9), 094015. <https://doi.org/10.1088/1748-9326/aa4bb9>

- Xie, S.-P., & Carton, J. A. (2004). Tropical Atlantic variability: Patterns, mechanisms, and impacts. *Earth's Climate: The Ocean-Atmosphere Interaction, Geophys. The Monograph, 147*, 121–142.
- Yan, Y., Li, L., & Wang, C. (2017). The effects of oceanic barrier layer on the upper ocean response to tropical cyclones. *Journal of Geophysical Research: Oceans, 122*(6), 4829–4844. <https://doi.org/10.1002/2017JC012694>
- Yoon, J.-H., & Zeng, N. (2010). An Atlantic influence on Amazon rainfall. *Climate Dynamics, 34*(2), 249–264. <https://doi.org/10.1007/s00382-009-0551-6>
- Zeng, N., Yoon, J.-H., Marengo, J. A., Subramaniam, A., Nobre, C. A., Mariotti, A., & Neelin, J. D. (2008). Causes and impacts of the 2005 Amazon drought. *Environmental Research Letters, 3*(1), 014002. <https://doi.org/10.1088/1748-9326/3/1/014002>
- Zweng, M., Seidov, D., Boyer, T., Locarnini, M., Garcia, H., Mishonov, A., et al. (2019). *World Ocean Atlas 2018, volume 2: Salinity*.